



OPEN

## Low dose ionising radiation elicits MPTP comparable alterations in locomotor Function, oxidative balance and mitochondrial homeostasis in zebrafish embryos

Ezgi Cahide<sup>1</sup>, Aydas Bayramov<sup>1</sup>, Merih Beler<sup>2</sup>, Derya Cansiz<sup>3</sup>, Ismail Unal<sup>3</sup>, Gizem Egilmez<sup>2</sup>, Selma Yaltkaya<sup>1</sup>, Atakan Karagoz<sup>4</sup>, Hüseyin Gündüz<sup>5</sup>, Ebru Emekli-Alturfan<sup>6</sup> & Sebnem Ercalik Yalcinkaya<sup>1</sup>✉

Prenatal exposure to environmental factors including low-dose ionising radiation and neurotoxins may disrupt the oxidant-antioxidant balance. Our aim was to assess the effects of exposure to low-dose ionising radiation (LDIR) and 1-methyl-4-phenyl-1,2,3,6-tetrahydropyridine (MPTP), which is a neurotoxin used to model Parkinson's disease (PD), on developing zebrafish embryos, focusing on the oxidant-antioxidant system and markers of mitochondrial damage associated with PD. Zebrafish embryos were divided into four groups: control, LDIR, MPTP, and LDIR combined with MPTP (LDIR + MPTP). A dental x-ray unit (60 kVp, 7 mA) was used for the exposures. The 0.08 s LDIR exposure was measured as 0.065 mGy using optically stimulated dosimeters. At the end of 72 h after fertilization, locomotor activities, acetylcholine esterase (AChE) activity, oxidative stress and antioxidant status were assessed. Expressions of genes associated with in PD as markers of mitochondrial damage (*pink1*, *parkin*, *dj1* and *lrrk2*) were determined by RT-PCR. Developmental toxicity was observed in all exposure groups as evidenced by pericardial edema, yolk sac edema and spinal curvature. LDIR exposure in zebrafish embryos affected oxidative and mitochondrial stress markers, as well as locomotor activity and AChE as a marker of cognitive function at levels comparable to the MPTP exposure. Our study is the first to determine the effects of LDIR from a dental x-ray unit on the response to MPTP, and we aim to further elucidate the mechanism of these changes observed particularly in the LDIR + MPTP group.

**Keywords** Low-dose ionising radiation, 1-methyl-4-phenyl-1,2,3,6-tetrahydropyridine, Oxidative stress, Antioxidant, Locomotor activity

Dental diagnostic imaging is an integral part of the practice of dentistry and radiation doses have been reduced with the development of digital techniques<sup>1,2</sup>. Exposure to ionising radiation (IR) is harmful, although radiation-related health risks decrease at lower doses<sup>3</sup>. In view of the lifetime frequency of exposure to dental diagnostic x-rays, even a small increase in health risk would be of significant public health importance<sup>4</sup>, and repeated exposure may increase the risk of cancer<sup>5</sup>.

The mechanism of deleterious IR effects is strongly linked to increased oxidative stress in irradiated tissues<sup>6</sup>. IR is able to penetrate the cells of living organisms, where it induces the ionization of both organic and inorganic compounds<sup>7,8</sup>. Due to the high-water content in cells, the radiolysis of water molecules by IR is the main process that contributes to the increased formation of reactive oxygen species (ROS)<sup>9</sup>. ROS react rapidly with macromolecules, including proteins, nucleic acids and lipids, leading to cell dysfunction, and apoptotic cell

<sup>1</sup>Department of Oral and Maxillofacial Radiology, Faculty of Dentistry, Marmara University, Istanbul, Turkey.

<sup>2</sup>Institute of Health Sciences, Department Biochemistry, Marmara University, Istanbul, Turkey. <sup>3</sup>Department of Medical Biochemistry, Faculty of Medicine, Istanbul Medipol University, Istanbul, Turkey. <sup>4</sup>Vocational School of

Health Services, Fenerbahçe University, Istanbul, Turkey. <sup>5</sup>Epsilon Landauer Dosimeter Technologies, Istanbul, Turkey. <sup>6</sup>Department of Basic Medical Sciences, Faculty of Dentistry, Marmara University, Istanbul, Turkey. ✉email: sebnemer@rocketmail.com

death<sup>6</sup>. As a result of elevated oxidative stress, not only direct negative side effects, but also ROS-related diseases can develop. Therefore, it is particularly important to identify effective and safe prophylactic compounds to protect humans from IR damage<sup>10</sup>.

Parkinson's disease (PD), clinically characterized by tremor, bradykinesia and rigidity, is the second most common neurodegenerative disorder in the world. The disease involves loss of dopaminergic neurons in the substantia nigra pars compacta (SNc), leading to dopamine depletion at nerve terminals<sup>11</sup>. Multiple environmental and genetic factors play a key role in the etiology of PD<sup>12,13</sup>. Environmental factors influencing PD risk include mitochondrial toxins such as 1-methyl-4-phenyl-1,2,3,6-tetrahydropyridine (MPTP)<sup>14</sup> and IR<sup>13</sup>. Oxidative stress has also been linked to PD<sup>15</sup>, and IR induces oxidative stress causing neurobiological responses<sup>16</sup>.

MPTP is a neurotoxin that induces selective loss of dopaminergic neurons in the mammalian midbrain. In different model organisms, exposure to MPTP leads to the characteristic symptoms of PD<sup>17</sup>. MPTP exposure in zebrafish embryos has been shown to damage dopaminergic neurons and reduce the number of dopaminergic cells in the diencephalon<sup>18</sup>. In zebrafish, the dopaminergic system is well characterized both in the embryonic and adult stages. For this reason, zebrafish is a suitable model organism to study the molecular pathways in neurodevelopment and neurotoxicology, as well as to explore potential therapeutic agents<sup>19</sup>.

Environmental exposures during sensitive developmental windows in the embryonic phase can have lasting effects on the health<sup>20</sup>. Previous investigations have focused on elements such as DNA damage mechanisms in the adult organism, free radical generation, and elevated cancer markers at low doses of IR<sup>21</sup>. Cells with high levels of mitotic activity are known to be hypersensitive to radiation. Although organogenesis and especially neurogenesis in the early fetal period are the most susceptible periods of the fetus to radiation, research on LDIR exposure during the embryonic stage is limited<sup>22</sup>. Prenatal effects have been studied in animal models<sup>23</sup>.

We hypothesized that LDIR exposure in developing zebrafish embryos would cause oxidative stress and mitochondrial stress, similar to MPTP, and could affect the locomotor functions of the embryo, and that LDIR exposure prior to MPTP could also affect the response to MPTP in the organism. To determine the molecular mechanisms of the effect of LDIR and MPTP, molecules involved in the oxidant-antioxidant system (malondialdehyde, nitric oxide, superoxide dismutase, glutathione S-transferase, glutathione and catalase) and activity of acetylcholinesterase were evaluated to determine cholinergic effects. In addition, to assess whether MPTP and IR induced changes in mitochondrial stress-related genes associated with PD, the expressions of *pink1*, *parkin*, *dj1*, and *lrrk2* were determined.

## Methods

### Chemicals tested

MPTP (purity  $\geq 98\%$ ) was purchased from Sigma-Aldrich, St Louis, MO, USA. It was analytical grade with the highest purity available.

### Maintenance of zebrafish

Wild-type AB/AB strain zebrafish were maintained under apparently disease-free conditions. Animal husbandry and spawning were performed in accordance with the relevant guidelines and regulations and the protocols approved by the University of Marmara Institutional Animal Care and Use Committee. Fish were kept in an aquarium rack system (Zebtec, Tecniplast, Italy) at  $27 \pm 1$  °C under a light/dark cycle of 14/10-hour and they were fed with commercial flake fish food complemented with live Artemia twice a day. The pH of system water ranges from 6.9 to 7.2. Reverse osmosis water that contains  $0.018 \text{ mg L}^{-1}$  Instant Ocean™ salt was used for all experiments. Zebrafish embryos (AB/AB) were obtained from the Zebrafish Research Laboratory in Marmara University and maintained in E3 medium. After natural spawnings, fertilized embryos were gathered and staged according to their developmental and morphology as described before<sup>24</sup>. We used zebrafish embryos up to 72 hpf and the European Commission Directive 2010/63/EU, permits experimentation in fish embryos at earliest life stages without being regulated as animal experiments; zebrafish are considered models *in vitro* until 120 hpf (<http://data.europa.eu/eli/dir/2010/63/2019-06-26>; accessed 21 May 2025 EFSA opinion: <https://doi.org/10.2903/j.efsa.2005.292>; accessed 21 May 2025). Care was taken to minimize the numbers of embryos used in the experiments in accordance with the ARRIVE guidelines.

### Embryo exposure

Zebrafish embryos of the AB/AB strain were selected under the stereomicroscope after fertilisation and divided into four groups including control group, MPTP-exposed group, LDIR- exposed group and MPTP-exposed combined with LDIR-exposed group.

The dental x-ray unit, Belmont AR-33RK5EU (Osaka, Japan), (60 kVp, 7 mA) with long cone (30 cm) and 4 mm Al filter was used for the low-dose ionizing radiation exposure. The MPTP, LDIR, and LDIR + MPTP groups were exposed to 0,08 s of x-ray, 800  $\mu\text{M}$  MPTP, and 0,08 s of x-ray before 800  $\mu\text{M}$  MPTP, respectively, at 24 h post-fertilization. Developmental parameters were monitored and documented daily under a stereomicroscope (Zeiss Discovery V8, Germany) until 72 hpf.

During the experiment, an optically stimulated (OSL) dosimeter (Epsilon Landauer, Istanbul, Turkey) was used for each exposure group (LDIR and LDIR + MPTP groups). These dosimeters had a sensitivity range of 0,05 mGy to 10,0 Gy with an uncertainty of 8% for deep and shallow dose Hp, which was done to compare the reliability of dose measurements. Each OSL dosimeter was placed in the centre of a petri dish to measure absorbed doses. The same conditions but without embryos were used to expose of two other OSL dosimeters. This procedure was repeated for each x-ray group. One dosimeter in each group was not exposed and served as

a control. The exposed OSls were then processed using an InLight Auto200 reader (Epsilon Landauer, Istanbul, Turkey) and the numbers read by the reader were recorded.

Developmental parameters were monitored using a stereomicroscope (ZEISS Discovery V8, Germany) and recorded daily until 72 hpf.

### Locomotor activity

The locomotor activity of the zebrafish embryos at 72 hpf was evaluated as described previously<sup>25</sup>. This was performed by placing a 60 mm Petri dish containing embryo medium on top of the motility wheel which is on the microscope stage. Then, by using an embryo poker tool the zebrafish embryo was positioned in the middle of the motility wheel and the time it took for an embryo to swim a predetermined distance was recorded and the average escape response was calculated.

### Biochemical assays

Zebrafish embryos were prepared as replicate pools of 72 hpf zebrafish. For each pool 100 embryos were homogenized in 1 ml PBS, followed by centrifuging briefly. The supernatant was used for the determination of biochemical parameters<sup>26</sup>.

#### Total protein assay

The method of Lowry was used to determine the levels of total proteins in the samples<sup>27</sup>. In this method, proteins first react with copper ions in an alkali medium and then they are reduced by Folin reagent. The absorbances are determined at 500 nm. The total protein levels were calculated and used to present the results per protein.

#### Lipid peroxidation assay

The method of Yagi was used to determine malondialdehyde (MDA) levels, the end product of lipid peroxidation (LPO), as thiobarbituric acid reactive substances. The extinction coefficient of  $1.56 \times 105 \text{ M}^{-1} \text{ cm}^{-1}$  was used LPO was expressed in terms of MDA equivalents as nmol MDA/mg protein<sup>28</sup>.

#### Nitric oxide assay

Nitric oxide (NO) was determined through the reduction of nitrate to nitrite by vanadium (III) chloride. The colored complex was measured at 540 nm with a spectrophotometer and the results were expressed as nmol NO/mg protein<sup>29</sup>.

#### Glutathione-S-Transferase assay

The activity of glutathione-S-transferase (GST) was determined spectrophotometrically at 340 nm and the absorbance of the product formed by GSH and 1-chloro-2,4-dinitro-benzenin (CDNB) conjugation was evaluated<sup>30</sup>.

#### Superoxide dismutase assay

Superoxide dismutase (SOD) activity was determined using the method based on the ability of SOD to increase the effect of riboflavin-sensitized photo-oxidation of O-dianisidine. Superoxide activity is produced by illuminating the reaction mixture containing O-dianisidine dihydrochloride and riboflavin by the light of a fluorescent lamp. The oxidation of O-dia-nisidine is sensitized by riboflavin and enhanced by SOD and the increase is linearly dependent on the concentration of SOD. Absorbances at 0 and 8th min of the illumination were measured using a spectrophotometer at 460 nm and the net absorbances were calculated. The results were expressed as U/mg protein<sup>31</sup>.

#### Glutathione (GSH) assay

The amount of glutathione (GSH) in the samples was measured using Beutler's method (1975), and the results are expressed as percentage GSH<sup>32</sup>.

#### Acetylcholinesterase (AChE) assay

The Ellman et al. method was used to measure the activity of acetylcholinesterase in the supernatants<sup>33</sup>. Acetylcholinesterase generates thiocholine in this mechanism, which combines with 5,5'-dithiobis (2-nitrobenzoic acid) to produce a yellow hue. At 412 nm, the yellow color's intensity is evaluated and directly correlated with the sample's enzyme activity.

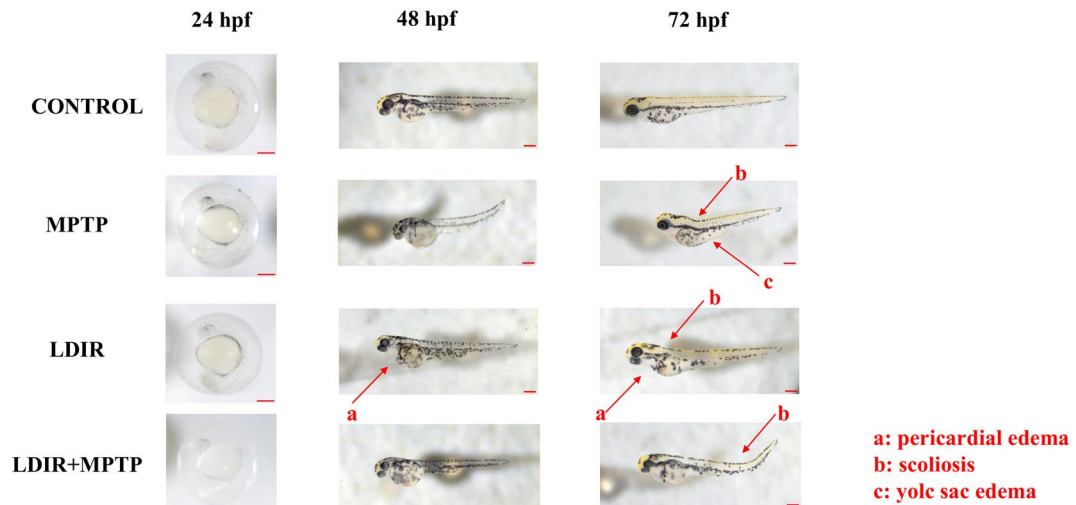
#### Catalase assay

Using Aebi's approach, the catalase activity was assessed in this study. The technique assesses the enzyme's ability to convert hydrogen peroxide into water<sup>34</sup>.

#### Reverse transcription (cDNA synthesis) and quantitative real-time PCR

For RT-PCR analysis, zebrafish embryos were prepared as replicate pools, and each pool consisted of 50 embryos. RNA was isolated from the embryos. Rneasy Mini Kit and Qiacube (Qiagen, Hilden, Germany) were used according to the instructions of the manufacturer. A single-stranded complementary DNA (cDNA) was obtained from 1 lg of total RNA using RT2 First Strand Kit (Qiagen, Hilden, Germany). DNA Master SYBR Green kit (Qiagen, Hilden, Germany) was used to perform RT-PCRs. The beta-actin is housekeeping gene and was used as a reference gene. Relative levels of transcription were calculated using the DD CT method based on the normalization of the values using the housekeeping gene<sup>35</sup>. The list of the primers used is shown in Table 1.

<i>dat</i>	forward primer 5'- TCACTGCCACGATGCCGTAT-3' reverse primer 5'- ACACCAAACCCGACTCCCAG-3'
<i>th.</i>	forward primer 5'- ATCTGTACACGACCCACGCC-3' reverse primer 5'- TGCCACTGGCCTCAACTGAA-3'
<i>lrrk2</i>	forward primer 5'-CCCTAAACCGCAGAGTATCA-3' reverse primer 5' -ATTCATAGTCCACCGGTCTG-3'
<i>pink1</i>	forward primer 5' -GGCAATGAAGATGATGTGGAAC-3' reverse primer 5'-GGTCGGCAGGACATCAGGA-3'
<i>dj1</i>	forward primer 5'-GGCCGGTAAAAGAGCGTTAG-3' reverse primer 5'-ACCCATGAGTCCTCCACTA-3'
<i>parkin</i>	forward primer 5'-GCGAGTGTCTGAGCTGAA-3' reverse primer 5'-CACACTGGAACACCCAGCACT-3'

**Table 1.** Forward and reverse primers used in the study.**Fig. 1.** Representative images of the zebrafish embryos in the groups. C: Control; MPTP: MPTP-exposed group; LDIR: LDIR-exposed group; LDIR + MPTP: MPTP-exposed combined with LDIR-exposed group.

### Statistical analysis

The effects of low-dose ionizing radiation and MPTP on zebrafish embryos were assessed using one-way analysis of variance (ANOVA) test and Dunn's multiple comparison test was used as a post-hoc test to compare the effects of MPTP on low dose IR exposed embryos. Statistical analysis was performed using GraphPad Prism 10 and  $p < 0.05$  was considered significant.

## Results

### Absorbed dose

Individual dose measurements were obtained by averaging the exposures within each LDIR group. The deep-dose equivalent (DDE) and shallow doses for the LDIR exposed group were both 0.065 mGy.

### Developmental analyses

The representative images of the zebrafish embryos are presented in Fig. 1, and quantitative assessment of developmental effects are presented in Table 2. Pericardial edema was observed in the LDIR exposed embryos at 48 and 72 hpf as denoted by the red arrow in Fig. 1. Since the pericardium surrounds and protects the growing heart, edema in this area may indicate disturbance of embryonic osmoregulation and problems with cardiovascular development<sup>36</sup>. Because the appearance and structure of zebrafish spines closely resemble those of humans, they offer special benefits for simulating human scoliosis. In our study, LDIR and MPTP caused scoliosis both when applied separately and together. Yolk sac edema was observed in MPTP group which indicates a significant influence on the development of the embryo as edema in the yolk sac is a known sign of physiological stress and disturbances in the homeostasis of the embryo<sup>37</sup>.

48 hpf	Control	MPTP	LDI	LDI + MPTP
Number of embryos	100	100	100	100
Pericardial edema	0	0	5	0
72 hpf				
Pericardial edema	0	0	5	0
Scoliosis	0	4	2	5
Yolk sac edema	0	5	0	0

**Table 2.** Quantitative assessment of developmental effects of MPTP and LDI in zebrafish embryos.

### Locomotor activities

Average speed, total distance swam and explored areas were determined to evaluate the effects of low dose ionising radiation and MPTP on locomotor activity. One-way ANOVA revealed significant differences in the average speed among treatment groups ( $F(3,36) = 414.9, p < 0.0001, \eta^2 = 0.97$ ), indicating a large effect size. Compared to the control group average speed significantly decreased in MPTP (95% CI: 267.0 to 320.3,  $p < 0.0001$ ); LDI (95% CI: 158.3 to 211.5,  $p < 0.0001$ ); and LDI + MPTP groups (95% CI: 281.8 to 335.0,  $p < 0.0001$ ). Decreased average speed was also found in the MPTP (95% CI: -135.3 to -82.10,  $p < 0.0001$ ) and LDI + MPTP groups (95% CI: -135.3 to -82.10,  $p < 0.0001$ ) compared to the LDI group (95% CI: 96.88 to 150.1,  $p < 0.0001$ ).

Significant difference was found in the total distance among treatment groups ( $F(3,36) = 95.08, p < 0.0001, \eta^2 = 0.88$ ). Total distance swam was found to be decreased in MPTP (95% CI: 381.9 to 562.8,  $p < 0.0001$ ); LDI (95% CI: 115.0 to 295.9,  $p < 0.0001$ ); and LDI + MPTP groups (95% CI: 390.2 to 571.1,  $p < 0.0001$ ) compared to the Control group. Total distance also decreased in the MPTP (95% CI: 357.3 to -176.4,  $p < 0.0001$ ) and LDI + MPTP groups (95% CI: 184.8 to 365.7,  $p < 0.0001$ ) compared to the LDI group.

According to the One-way ANOVA significant differences were found in the explored areas among treatment groups ( $F(3,36) = 99.37, p < 0.0001, \eta^2 = 0.89$ ). Decreased explored areas was detected in the MPTP (95% CI: 8.329 to 12.47,  $p < 0.0001$ ); LDI (95% CI: 1.129 to 5.271,  $p = 0.001$ ) and LDI + MPTP groups (95% CI: 8.329 to 12.47,  $p < 0.0001$ ) compared to the Control group. Moreover, explored areas of the MPTP (95% CI: -9.271 to -5.129,  $p < 0.0001$ ) and LDI + MPTP (95% CI: 5.729 to 9.871,  $p < 0.0001$ ) groups was significantly lower than the LDI group (Fig. 2).

### Oxidant-antioxidant analyses

Figure 3A shows the outcomes of lipid peroxidation analyses for the control, MPTP, LDI, and LDI + MPTP groups. One-way ANOVA revealed significant differences in LPO levels among treatment groups ( $F(3,8) = 64.43, p < 0.0001, \eta^2 = 0.96$ ), indicating a large effect size. Increased malondialdehyde (MDA) concentrations indicated the activation of lipid peroxidation in the MPTP (95% CI: 0.5792 to -0.2741,  $p < 0.0001$ ), LDI (95% CI: 0.3139 to -0.008781,  $p = 0.0386$ ), and LDI + MPTP (95% CI: 0.7592 to -0.4541,  $p < 0.0001$ ) groups compared to the control group. Moreover when compared with the LDI group, MDA were significantly higher in the MPTP (95% CI: 0.1128 to 0.4179,  $p = 0.0024$ ) and LDI + MPTP groups (95% CI: 0.5979 to -0.2928,  $p < 0.0001$ ).

The results of Glutathione S-Transferase (GST) analyses of the control, MPTP, LDI, and LDI + MPTP groups are shown in Fig. 3B. Significant differences in GST activities were observed among treatment groups ( $F(3,8) = 69.44, p < 0.0001, \eta^2 = 0.96$ ), indicating a large effect size. GST activity increased in response to MPTP (95% CI: -8.516 to -5.267,  $p < 0.0001$ ) and LDI + MPTP treatments (95% CI: -5.244 to -1.995,  $p = 0.0005$ ) indicating the activation of detoxification mechanisms. The highest increase in GST activity was seen in the MPTP group, which was statistically higher than the LDI (95% CI: 3.777 to 7.027,  $p < 0.0001$ ) and LDI + MPTP groups (95% CI: 1.647 to 4.897,  $p = 0.0009$ ).

The results of CAT analyses of the control, MPTP, LDI and LDI + MPTP groups are shown in Fig. 3C.

One-way ANOVA revealed significant differences in CAT activities among treatment groups ( $F(3,8) = 66.51, p < 0.0001, \eta^2 = 0.96$ ). CAT activities decreased significantly in the MPTP (95% CI: 23.95 to 58.84,  $p = 0.0003$ ) and LDI (95% CI: 5.666 to 40.56,  $p = 0.0121$ ) groups compared to the control group, as an indicator of decreased ability to disproportionate hydrogen peroxide. On the other hand, in the LDI + MPTP group, CAT activities were significantly higher than the control (95% CI: 48.87 to -13.97,  $p = 0.0019$ ), LDI (95% CI: -71.98 to -37.09,  $p < 0.0001$ ), and MPTP groups (95% CI: -90.26 to -55.37,  $p < 0.0001$ ).

Significant differences in SOD activities were observed among treatment groups ( $F(3,8) = 92.94, p < 0.0001, \eta^2 = 0.97$ ). Indicating the activation of oxidoreductase activity to dismutate the superoxide anion, SOD activity increased significantly in the MPTP (95% CI: -3.247 to -2.181,  $p < 0.0001$ ), LDI (95% CI: -1.585 to -0.5199,  $p = 0.001$ ), and LDI + MPTP (95% CI: -2.178 to -1.113,  $p < 0.0001$ ) groups compared to the control group. SOD activity was significantly higher in the MPTP group than the LDI (95% CI: 1.129 to 2.194,  $p < 0.0001$ ) and LDI + MPTP groups (95% CI: 0.5359 to 1.601,  $p = 0.0009$ ). On the other hand, in the LDI + MPTP group SOD activity was significantly higher than the LDI group (95% CI: -1.125 to -0.05986,  $p = 0.03$ ) (Fig. 3D).

The results of GSH analyses of the control, MPTP, LDI and LDI + MPTP groups are shown in Fig. 3E.

GSH levels were found to be significantly different among treatment groups ( $F(3,8) = 46.79, p < 0.0001, \eta^2 = 0.95$ ). GSH levels decreased significantly in the MPTP (95% CI: 0.5460 to 0.9787,  $p < 0.0001$ ) and LDI groups (95% CI: 0.1440 to 0.5767,  $p = 0.003$ ) compared to the control group. GSH levels of the LDI group were significantly higher than the MPTP group (95% CI: -0.6184 to -0.1856,  $p = 0.0015$ ) and GSH levels in the LDI + MPTP group were significantly higher than the MPTP group (95% CI: -0.8030 to -0.3703,  $p = 0.0001$ ) (Fig. 3E).

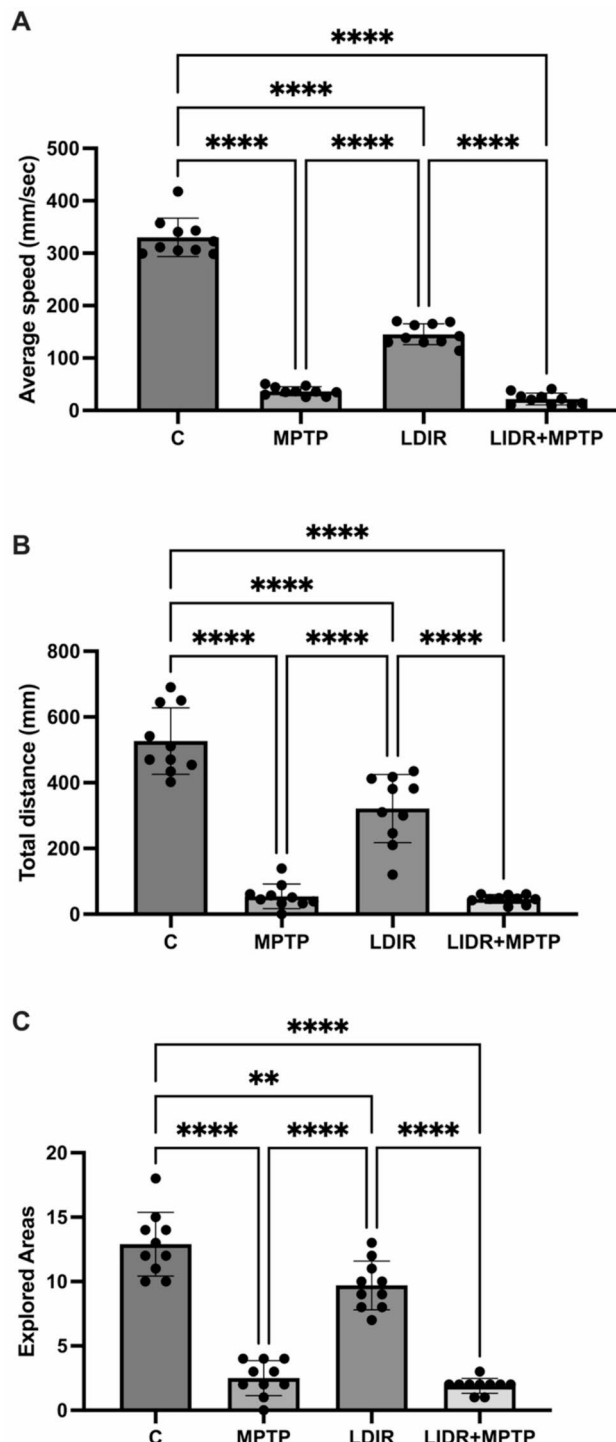


**Fig. 2.** (A) Average speed (mm/sec); (B) Total distance swam (mm); (C) Explored areas (%) of the groups. \* $p < 0.05$ ; \*\* $p < 0.01$ ; \*\*\* $p < 0.001$ ; \*\*\*\* $p < 0.0001$ . Data are expressed as mean  $\pm$  SD,  $n = 10$ . C: Control group; MPTP: 1-methyl-4-phenyl-1,2,3,6-tetrahydropyridine exposed group; LDIR: low dose ionising radiation exposed group; LDIR + MPTP: MPTP combined with LDIR exposed group; SD: Standard deviation.

#### AChE analysis

The results of Acetylcholine esterase (AChE) analyses of the control, MPTP, LDIR and LDIR + MPTP groups are shown in Fig. 4A. One-way ANOVA revealed significant differences in AChE activities in the treatment groups ( $F(3,8) = 58.96, p < 0.0001, \eta^2 = 0.96$ ). AChE activity decreased significantly in the, MPTP (95% Cl: 0.1376 to 0.2552,  $p < 0.0001$ ), LDIR (95% Cl: 0.04924 to 0.1668,  $p = 0.0017$ ), and LDIR + MPTP (95% Cl: 0.1608 to 0.2784,  $p < 0.0001$ ) groups as a sign that cholinergic functions are affected. In the LDIR group, AChE activity was

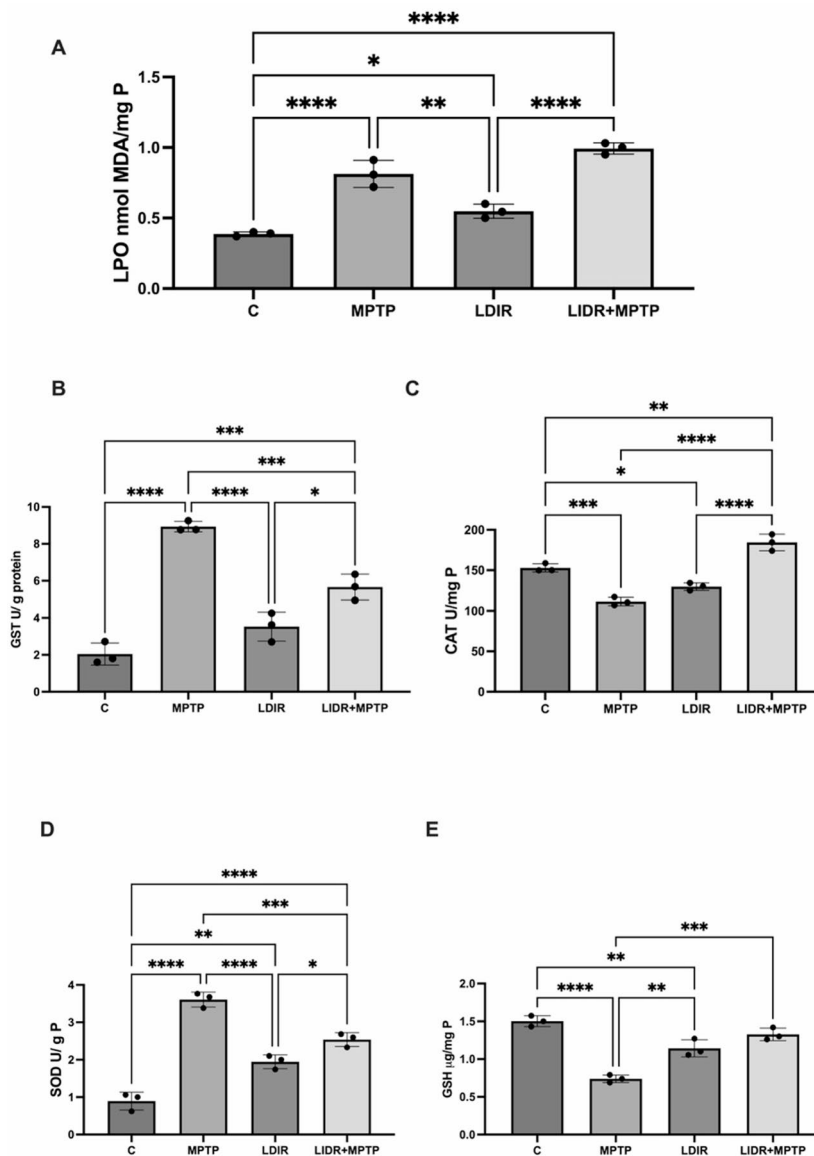


**Fig. 3.** (A) Malondialdehyde (MDA) levels as an index of lipid peroxidation (LPO); (B) Glutathione S-transferase (GST) activities of the groups; (C) Catalase (CAT) activities of the groups; (D) Superoxide dismutase (SOD) activities of the groups; (E) Glutathione (GSH) levels of the groups. \* $p < 0.05$ ; \*\* $p < 0.01$ ; \*\*\* $p < 0.001$ ; \*\*\*\* $p < 0.0001$ . Data are expressed as mean  $\pm$  SD from the three independent experiments. C: Control group; MPTP: 1-methyl-4-phenyl-1,2,3,6-tetrahydropyridine exposed group; LDIR: low-dose ionising radiation exposed group; LDIR + MPTP: MPTP combined with LDIR exposed group; SD: Standard deviation.

significantly higher than the MPTP (95% CI: 0.1471 to 0.02954,  $p = 0.0058$ ) and LDIR + MPTP (95% CI: 0.05277 to 0.1704,  $p = 0.0013$ ) groups.

### NO analysis

The results of nitric oxide (NO) analyses in the control, MPTP, LDIR and LDIR + MPTP groups are shown in Fig. 4B. Differences were found in the GST activities among treatment groups ( $F(3,8) = 70.11$ ,  $p < 0.0001$ ,  $\eta^2 = 0.96$ ). As a potent oxidant, NO levels increased significantly in the MPTP (95% CI: - 1.659 to - 0.6655,  $p = 0.0003$ ), LDIR 95% CI: - 1.000 to - 0.0065,  $p = 0.0471$ ), and LDIR + MPTP groups (95% CI: - 2.624 to - 1.630,  $p < 0.0001$ ) compared to the control group. NO levels in the LDIR + MPTP group were significantly higher than the MPTP (95% CI: - 1.461 to - 0.4675,  $p = 0.0012$ ) and LDIR groups (95% CI: - 2.120 to - 1.126,  $p < 0.0001$ ).

### Gene expression analysis

In our study, the expressions of dopamine transporter (dat) and tyrosine hydroxylase (th) were assessed as critical indicators of mitochondrial stress associated with neurodegeneration induced by MPTP exposure.

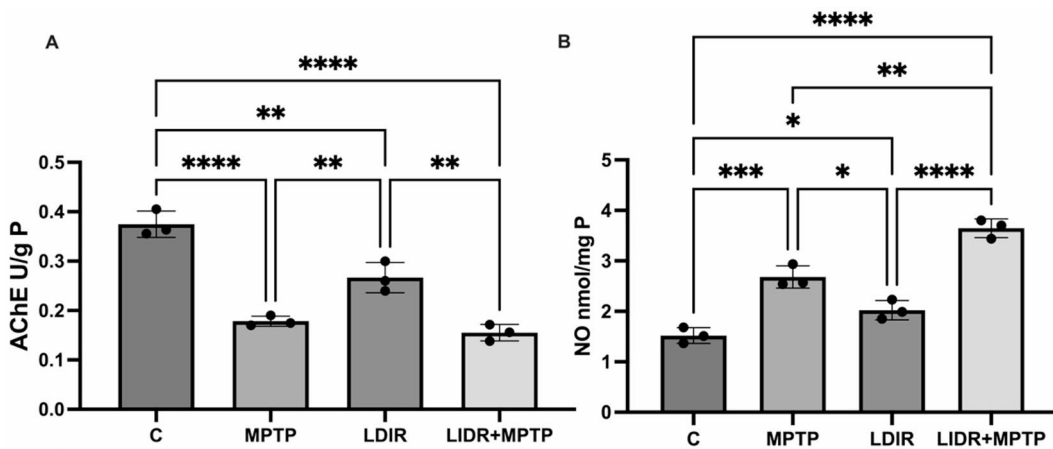


**Fig. 4.** (A) Acetylcholine esterase activities (AChE) of the groups (B) Nitric oxide (NO) levels of the groups. \* $p < 0.05$ ; \*\* $p < 0.01$ ; \*\*\* $p < 0.001$ ; \*\*\*\* $p < 0.0001$ . Data are expressed as mean  $\pm$  SD from the three independent experiments. C: Control group; MPTP: 1-methyl-4-phenyl-1,2,3,6-tetrahydropyridine exposed group; LDIR: low dose ionising radiation exposed group; LDIR + MPTP: MPTP combined with LDIR exposed group; SD: Standard deviation.

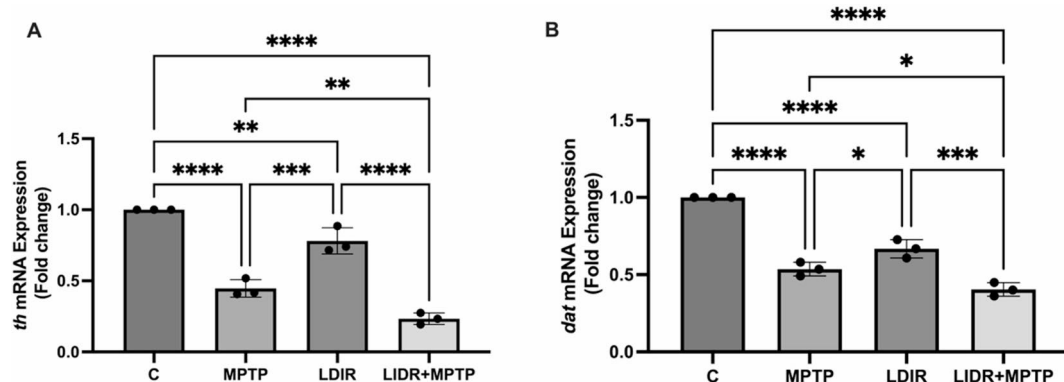


**Fig. 5.** Bar graph presentation of the fold change of (A) *th* and (B) *dat* transcripts quantified by RT-PCR. All RT-PCR results are normalized to *b*-actin, the housekeeping gene and expressed as change from their respective controls. Data are expressed as mean  $\pm$  SD from the three independent experiments. \* $p < 0.05$ ; \*\* $p < 0.01$ ; \*\*\* $p < 0.001$ ; \*\*\*\* $p < 0.0001$  SD: Standard deviation. C: Control group; MPTP: 1-methyl-4-phenyl-1,2,3,6-tetrahydropyridine exposed group; LDIR: low dose ionising radiation exposed group; LDIR + MPTP: MPTP combined with LDIR exposed group. SD: Standard deviation.

Significant differences in *th* expressions among treatment groups were observed ( $F(3,8) = 101, p < 0.0001, \eta^2 = 0.97$ ). Decreased expressions of *th* were found in the MPTP (95% CI: 0.3991 to 0.7067,  $p < 0.0001$ ), LDIR (95% CI: 0.06532 to 0.3729,  $p = 0.008$ ), and LDIR + MPTP groups (95% CI: 0.6126 to 0.9202,  $p < 0.0001$ ). *Th* is a key enzyme in the dopaminergic pathway and decreased *th* expression indicate impaired dopaminergic functions, especially in the LDIR + MPTP group. *th* expression of the LDIR + MPTP group was significantly lower than the MPTP (95% CI: 0.05964 to 0.3673,  $p = 0.0093$ ) and LDIR groups (95% CI: 0.3934 to 0.7010,  $p < 0.0001$ ) (Fig. 5A).

Similarly, one-way ANOVA revealed significant differences in *dat* expressions among treatment groups ( $F(3,8) = 106.9, p < 0.0001, \eta^2 = 0.98$ ). *dat* expressions also decreased in the MPTP (95% CI: 0.3520 to 0.5762,  $p < 0.0001$ ), LDIR (95% CI: 0.2203 to 0.4445,  $p < 0.0001$ ) and LDIR + MPTP groups (95% CI: 0.4841 to 0.7082,  $p < 0.0001$ ). Both MPTP and LDIR treatments affected *dat* expressions indicating impaired dopamine reuptake and disrupted dopaminergic signaling. Similar to *th* expression, *dat* expression of the LDIR + MPTP group was significantly lower than the MPTP (95% CI: 0.01998 to 0.2441,  $p = 0.0226$ ) and LDIR groups (95% CI: 0.1517 to 0.3758,  $p = 0.0003$ ) (Fig. 5B).

The mRNA expression levels of *pink1* of the groups are shown in Fig. 6A. *pink1* expressions were significantly different among treatment groups ( $F(3,8) = 45.55, p < 0.0001, \eta^2 = 0.94$ ). Indicating mitochondrial damage, *pink1* expression increased significantly in the MPTP (95% CI: -2.491 to -0.6672,  $p = 0.0024$ ), LDIR (95% CI: -4.231 to -2.407,  $p < 0.0001$ ), and LDIR + MPTP (95% CI: -2.340 to -0.5156,  $p = 0.0046$ ) groups compared to the control group. *pink1* expression was significantly higher in the LDIR group when compared to the MPTP group (95% CI: -2.651 to -0.8273,  $p = 0.0013$ ) and LDIR + MPTP group (95% CI: 0.9790 to 2.803,  $p = 0.0007$ ).

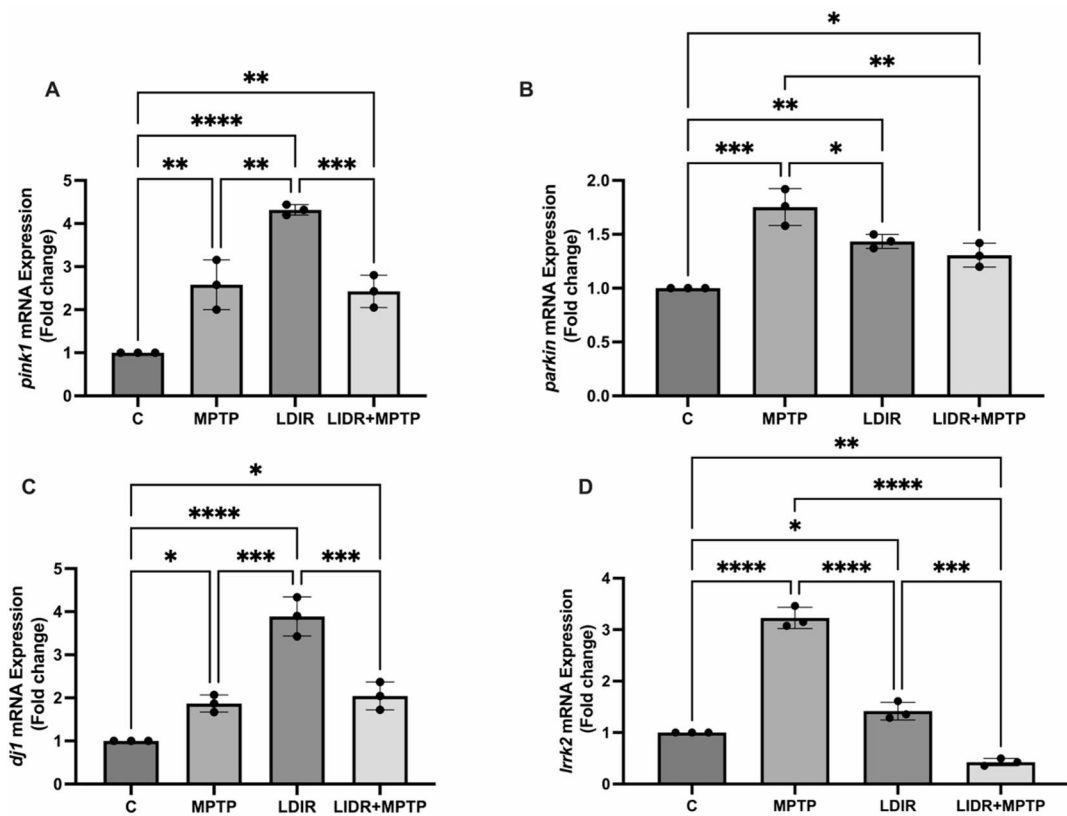


**Fig. 6.** Bar graph presentation of the fold change of (A) *pink1*, (B) *parkin*, (C) *dj1* and (D) *lrrk2* transcripts quantified by RT-PCR. All RT-PCR results are normalized to b-actin, the housekeeping gene and expressed as change from their respective controls. \* $p < 0.05$ ; \*\* $p < 0.01$ ; \*\*\* $p < 0.001$ ; \*\*\*\* $p < 0.0001$ . Data are expressed as mean  $\pm$  SD from the three independent experiments C: Control group; MPTP: 1-methyl-4-phenyl-1,2,3,6-tetrahydropyridine exposed group; LDIR: low dose ionising radiation exposed group; LDIR + MPTP: MPTP combined with LDIR exposed group, SD: Standard deviation.

One-way ANOVA showed significant differences in *parkin* expressions among treatment groups ( $F(3,8) = 26.62$ ,  $p < 0.0001$ ,  $\eta^2 = 0.91$ ). *parkin* expression increased significantly in the LDIR (95% Cl:  $-0.7140$  to  $-0.1560$ ,  $p = 0.0047$ ), MPTP (95% Cl:  $-1.032$  to  $-0.4739$ ,  $p = 0.0001$ ), and LDIR + MPTP (95% Cl:  $-0.5856$  to  $-0.02769$ ,  $p = 0.0321$ ) groups showing the upregulated PINK1/Parkin pathway. In addition, when compared to the LDIR and LDIR + MPTP groups, the *parkin* expression of the MPTP group was significantly higher (95% Cl:  $0.03889$  to  $0.5968$ ,  $p = 0.0268$  and 95% Cl:  $0.1672$  to  $0.7252$ ,  $p = 0.0040$ , respectively) (Fig. 6B).

*dj1* expressions differed significantly among treatment groups ( $F(3,8) = 50.58$ ,  $p < 0.0001$ ,  $\eta^2 = 0.95$ ). In response to increased oxidative stress, *dj1* expressions increased significantly in the MPTP (95% Cl:  $-1.644$  to  $-0.09713$ ,  $p = 0.0285$ ), LDIR (95% Cl:  $-3.661$  to  $-2.115$ ,  $p < 0.0001$ ), and LDIR + MPTP (95% Cl:  $-1.818$  to  $-0.2720$ ,  $p = 0.0108$ ) groups as a redox-sensitive chaperone. *dj1* expression was significantly higher in the LDIR group, compared to the MPTP (95% Cl:  $-2.791$  to  $-1.245$ ,  $p = 0.0001$ ) and LDIR + MPTP groups (95% Cl:  $1.070$  to  $2.616$ ,  $p = 0.0003$ ) (Fig. 6C).

The results of *lrrk2* expression analyses of the control, MPTP, LDIR, and LDIR + MPTP groups are shown in Fig. 6D. Significant differences in *lrrk2* expressions were found among treatment groups ( $F(3,8) = 228.3$ ,  $p < 0.0001$ ,  $\eta^2 = 0.98$ ), indicating a large effect size. *lrrk2* expressions were significantly increased in the MPTP (95% Cl:  $-2.591$  to  $-1.866$ ,  $p < 0.0001$ ) and LDIR groups (95% Cl:  $-0.7802$  to  $-0.05433$ ,  $p = 0.0257$ ) compared to the control group.

MPTP group, *lrrk2* expression was significantly higher than the LDIR (95% Cl:  $1.448$  to  $2.174$ ,  $p < 0.0001$ ) and LDIR + MPTP groups (95% Cl:  $2.440$  to  $3.166$ ,  $p < 0.0001$ ). In addition, *lrrk2* expression was significantly lower in the LDIR + MPTP group than in the LDIR group (95% Cl:  $0.6287$  to  $1.355$ ,  $p < 0.0001$ ).

## Discussion

Ionising radiation; mainly x-rays, is used in the dental radiodiagnostics. Our study is the first to show that low-dose ionizing radiation can induce comparable effects to MPTP by activating the expression of PD genes associated with mitochondrial damage, in developing zebrafish embryos. The results of our study showed that LDIR exposure in zebrafish embryos altered oxidative and mitochondrial stress markers, as well as locomotor and cognitive function markers at levels comparable to MPTP exposure.

Environmental exposures such as LDIR or MPTP can have adverse effects on health during the embryonic phase, a sensitive stage of development<sup>20</sup>. MPTP is a neurotoxin that has been shown to induce a selective loss of dopaminergic neurons in the mammalian midbrain, leading to characteristic symptoms of PD in various animal models including zebrafish<sup>19</sup>. Several studies showed that MPTP exposure reduces locomotor activity in zebrafish embryos<sup>18,38</sup>. In our study a significant decrease in locomotor activity was observed in all exposure groups, as evidenced by decreased average speed, total distance and areas explored. On the other hand, malformations such as yolk sac edema, pericardial edema, and scoliosis observed in embryos may be suggested to have a potential impact on locomotor activity. As shown in Table 1, these malformations were observed in a maximum of 5% of embryos exposed to MPTP and LDIR. Yolk sac edema may affect energy metabolism by impairing osmoregulation and nutrient absorption, while pericardial edema may impair the circulatory system, limiting locomotor capacity<sup>39</sup>. Scoliosis may also affect neuromuscular coordination, leading to a decrease in swimming behavior<sup>40</sup>. However, the low prevalence of these malformations suggests that locomotor changes are primarily due to the neurotoxic effects of MPTP on dopaminergic neurons and the disruption of neuronal function by LDIR via oxidative stress.

In our study, we observed that exposure to MPTP and LDIR caused a significant decrease in *dat* and *th* gene expressions in zebrafish embryos. These genes play a critical role in dopaminergic system function; *th* regulates dopamine synthesis, while *dat* controls synaptic dopamine reuptake. The decrease in these gene expressions leads to impaired dopaminergic neuron function and is associated with the observed decrease in locomotor function. It was also noteworthy that the decrease in locomotor activity was accompanied by a decrease in AChE activity which is a cholinergic enzyme. Our results are consistent with those of Cansiz et al. and Kollayan et al. who showed decreased AChE activity and decreased locomotor activity in zebrafish embryos treated with MPTP and LDIR, respectively<sup>41,42</sup>. The inhibition of locomotor activity in the LDIR group may be related to the deleterious effects of x-rays on cholinergic function<sup>43</sup>. While no difference was observed between the MPTP and LDIR + MPTP groups, the decrease was significant in the LDIR + MPTP group compared with the LDIR group, indicating that LDIR before neurotoxin exposure had no effect on locomotor activity.

When MPP<sup>+</sup> is taken by the dopaminergic neurons, it inhibits mitochondrial oxidative phosphorylation complex 1, leading to mitochondrial stress. Mitophagy is the process by which damaged mitochondria are targeted for lysosomal degradation. *pink1* and *parkin* work coordinately to regulate mitophagy<sup>38</sup>. Defects in *pink1/parkin* regulated mitophagy lead to the accumulation of damaged mitochondria which contributes to PD<sup>44</sup>. *pink1* has been shown to protect cells against oxidative stress induced apoptosis<sup>45</sup>. Increased *lrrk* and *pink1* expressions were found in MPTP exposed zebrafish embryos<sup>41</sup>. In a previous study, Ustundag et al. reported that *pink1*, *parkin* and *lrrk* expressions were significantly increased in the MPTP exposed zebrafish embryos<sup>38</sup>. As mitochondrial impairment activates *lrrk2* before the presence of neurodegeneration and *pink1* regulates mitophagy to target the damaged mitochondria for lysosomal degradation, increased *lrrk* and *pink1* expressions may indicate mitochondrial stress due to MPTP and LDIR exposures<sup>44,46</sup>. Consistent with these reports MPTP has shown to increase *pink1*, *parkin* and *lrrk* gene expression in zebrafish embryos.

*dj1* plays a role in antioxidative stress reactions and the loss of its function has been suggested to lead to the onset of PD<sup>47</sup>. Decreased *dj1* gene expressions was found in MPTP exposed zebrafish embryos<sup>38,41</sup>. In contrast to these studies, we found increased expressions of the *dj1* gene.

In our study, LDIR, MPTP and LDIR combined with MPTP exposure led to changes in the expression of *pink1*, *parkin*, *dj1* and *lrrk* genes as indicators of mitochondrial damage. The expression of *pink1*, *parkin* and *dj1* genes increased in all exposure groups compared to the control group. On the other hand, *lrrk* gene expression was found to be increased in the LDIR and MPTP groups, whereas a decrease was observed in the LDIR combined with MPTP exposure group. Our study is the first to show that LDIR may act like MPTP by activating the expressions of genes that regulate mitochondrial stress in developing zebrafish embryos.

One of the major causes of radiation-induced damage is the generation of ROS and free radicals as a result of radiation exposure. ROS react with tissues, causing LPO, DNA damages, and enzyme inactivation, all of which are radiation damage mediators<sup>48</sup>. Rats showed an increase in LPO levels following exposure to 3 Gy (Gy) of x-rays<sup>49</sup>. Consistent with this finding, our group has recently shown increased oxidative stress in low dose x-ray radiation exposed zebrafish embryos as evidenced by increased LPO<sup>42,48</sup>. Similarly, increased LPO levels were observed in LDIR-exposed zebrafish embryos in our study.

In the neurodegenerative diseases including PD, the generation of free radicals particularly ROS and RNS, is known to be detrimental, as they affect proteins, lipids, and nucleic acids<sup>50–52</sup>. The increase in ROSs damages the target neuronal cells<sup>53</sup> and dopaminergic neurons are more susceptible to oxidative stress. MPTP<sup>14</sup> and IR<sup>13</sup> are environmental factors that may influence the risk of PD by inducing oxidative stress on the neurobiological responses<sup>16</sup>. As a neurotoxin, MPTP has been shown to induce selective loss of dopaminergic neurons in the mammalian midbrain, leading to characteristic symptoms of PD in various animal models including zebrafish<sup>19,38</sup>. Zebrafish embryos have been shown to be susceptible to the dopaminergic neurotoxin MPTP<sup>18</sup>. When MPTP is metabolized by monoamine oxidase-B, 1-Methyl-4- phenylpyridinium (ion) (MPP<sup>+</sup>) is formed as the ultimate toxic agent<sup>38</sup>. The conversion of MPTP to MPP<sup>+</sup> has been shown to destroy the dopaminergic neurons by leading to the generation of hydroxyl radicals and causing LPO in experimental models<sup>54–59</sup>. Similarly in our study, increased LPO levels were observed in MPTP-exposed zebrafish embryos when compared with the control group.

Another free radical produced by irradiation is NO, which is a biological mediator in biochemical reactions<sup>60</sup>. After high-dose whole-body x-ray irradiation, *in vivo* NO generation was measured in mice, resulting in delayed NO synthase expression and NO formation<sup>61</sup>. Increased NO levels were found in rabbits after exposure to 550 rads of x-rays<sup>62</sup>. In previous studies from our zebrafish research laboratory, Karagoz et al. and Kollayan et al. found a significant increase in NO levels in LDIR-exposed zebrafish embryos<sup>42,48</sup>. A similar increase in NO levels was observed in the LDIR group. In addition, we observed a dramatic and significant increase in LPO and NO

levels in the LDIR combined with MPTP group compared to the LDIR group, indicating that MPTP treatment enhanced LPO and NO levels and increased oxidative stress in the LDIR-exposed zebrafish embryos.

In addition to being an endogenous free radical, NO is a potent vasodilator. The edema associated with radiation has been reported to indicate an increase in the permeability of the capillary wall. Vessel dilation is one of the most common early changes observed in the capillaries and pre-arterioles after irradiation<sup>42</sup>. Accordingly, increased NO levels in the ionizing radiation groups may be associated with the observed pericardial edema findings. Consistent with this, in our study the increase in NO levels was accompanied by a pericardial edema finding.

According to the oxidative stress hypothesis of PD, NO plays an important role in creating an environment that can damage the dopaminergic neurons<sup>63</sup>. The results of our study showed increased NO levels in MPTP-exposed zebrafish embryos. In a previous study, Cansiz et al. observed increased NO levels in MPTP-exposed zebrafish embryos, and our results were in agreement with their findings<sup>41</sup>. In addition, we observed a significant increase in NO levels in the LDIR + MPTP group compared to the MPTP and LDIR groups, suggesting an enhancement of the NO response by both treatments.

SOD can protect cells from the damaging effects of reactive oxygen species through the detoxification of superoxide radicals<sup>64</sup>. There are several reports on the role of SOD activities in the effect of LDIR<sup>65,66</sup>. Kojima et al. showed that SOD activity was increased in LDIR-exposed mice<sup>56</sup>. Increased SOD activity has also been reported in zebrafish embryos exposed to LDIR<sup>48</sup>. In the present study, we observed increased SOD activities in zebrafish embryos exposed to MPTP, LDIR and LDIR combined with MPTP. Increased levels of NO or LPO due to LDIR and MPTP exposure may be the reason for the increase in SOD activity.

Catalase is also an antioxidant enzyme that prevents hydroxyl radical generation and separates hydrogen peroxide into water and oxygen<sup>67</sup>. Few studies showed that environmental factors affect the CAT activity<sup>56,68</sup>. Kollayan et al. reported that dental x-ray exposure decreased CAT activities in zebrafish embryos<sup>42</sup>. We found decreased CAT activity in LDIR and MPTP exposed zebrafish embryos and when compared to the LDIR and MPTP groups an activation of CAT activity was observed in the LDIR combined with MPTP exposure group.

In our study, exposure to MPTP and LDIR caused changes in the activities of elements of the antioxidant defence system, as well as causing oxidative stress. We found decreased levels of GSH, which is the major antioxidant in cells, in MPTP and LDIR exposed zebrafish embryos. In accordance with our results Karagoz et al. reported decreased GSH levels in standard panoramic x-ray mode-exposed zebrafish embryos, however, in the same study increased GSH levels were found in the pedodontic panoramic x-ray mode-exposed group<sup>48</sup>. It has been reported that minor oxidative stress can boost intracellular GSH levels as an adaptive response, whereas severe oxidative stress might cause GSH levels to drop<sup>69</sup>. Exposure to MPTP has also been shown to decrease GSH levels<sup>70</sup>. The reason for the more dramatic decrease in GSH levels in the MPTP group compared to the LDIR group may be due to the higher LPO and NO, as indicators of oxidative stress in the MPTP group.

GST enzymes catalyse the conjugation of reduced glutathione to electrophilic groups on the substrate molecules to make the products of oxidative stress soluble for their easy elimination from the cell<sup>41,71</sup>. Previous studies have shown an increase in GST levels due to oxidative stress and environmental stimuli<sup>72,73</sup>. Transient overexpression of GST has been shown in MPTP-injected mice, suggesting that GST acts as an endogenous regulator of the cellular stress induced by MPTP to protect cells from ROS<sup>71</sup>. The expression and activity of GST were detected as early as 4 hpf in zebrafish embryos showing that GST enzymes are not only expressed but are also active during early embryogenesis<sup>74</sup>. Increased GST activities in x-ray exposed zebrafish embryos have been reported previously<sup>25,42</sup>. In accordance with these reports we found significant increases in the GST activities of the MPTP and LDIR combined with MPTP exposure groups. On the other hand, the increase in the GST activity of the LDIR group was not statistically significant. LDIR exposure before MPTP treatment decreased the GST response compared to the MPTP group, but increased it compared to the LDIR group.

In the practice of dental radiology, lower radiation doses are required for digital imaging sensors<sup>75</sup>. Considering our previous research, an exposure time of 0.08 s, which is one of the frequently used exposure settings in intraoral dental imaging, was chosen as a representative exposure time of LDIR<sup>42</sup>.

Our study is the first to determine the effects of LDIR from a dental diagnostic x-ray unit on the response to MPTP, focusing on the oxidant-antioxidant system and the expression of genes related with PD as markers of mitochondrial homeostasis. Based on our results, we may suggest that exposure to LDIR during the embryonic period may alter the response to neurotoxin treatment in terms of mitochondrial stress, oxidant-antioxidant status, locomotor and cholinergic functions in zebrafish embryos. On the other hand, the combined effects of LDIR and MPTP on oxidative damage and mitochondrial stress-related gene expression require further investigation with larger sample sizes to clarify their mechanisms.

## Data availability

The data that support the findings of this study are available from the corresponding author upon reasonable request.

Received: 5 May 2025; Accepted: 17 November 2025

Published online: 25 November 2025

## References

1. Hwang, S. Y. et al. Y. Health effects from exposure to dental diagnostic x-ray. *Environ. Health Toxicol.* **33**, 018017. <https://doi.org/10.5620/eht.e2018017> (2018).
2. Bahreyni Toossi, M. T., Akbari, F., Bayani & Roodi Radiation exposure to critical organs in panoramic dental examination. *Acta Med. Iranica.* **50**, 809–813 (2012).

3. Brenner, D. J. et al. Cancer risks attributable to low doses of ionizing radiation: Assessing what we really know. *Proc. Natl. Acad. Sci. USA* **100**, 13761–13766 (2003).
4. Crane, G. D. & Abbott, P. V. Radiation shielding in dentistry: An update. *Aust Dent J.* **61**, 277–281. <https://doi.org/10.1111/adj.12389> (2016).
5. Zielinski, J. M. et al. Low dose ionizing radiation exposure and cardiovascular disease mortality: Cohort study based on Canadian National dose registry of radiation workers. *Int. J. Occup. Med. Environ. Health* **22**, 27–33. <https://doi.org/10.2478/v10001-009-001-z> (2009).
6. Buonanno, M., de Toledo, S. M., Pain, D. & Azzam, E. I. Long-term consequences of radiation-induced bystander effects depend on radiation quality and dose and correlate with oxidative stress. *Radiat. Res.* **175**, 405–415. <https://doi.org/10.1667/RR2461.1> (2011).
7. Thiagarajan, A. & Yamada, Y. Radiobiology and radiotherapy of brain metastases. *Clin. Exp. Metastasis* **34**, 411–419. <https://doi.org/10.1007/s10585-017-9865-7> (2017).
8. Kirsch, D. G. et al. The future of radiobiology. *J. Natl Cancer Inst.* **110**, 329–340. <https://doi.org/10.1093/jnci/djx231> (2018).
9. Santacruz-Gomez, K. et al. Antioxidant activity of hydrated carboxylated nanodiamonds and its influence on water  $\gamma$ -radiolysis. *Nanotechnology* **29**, 125707. <https://doi.org/10.1088/1361-6528/aaa80e> (2018).
10. Burgio, E., Piscitelli, P. & Migliore, L. Ionizing radiation and human health: reviewing models of exposure and mechanisms of cellular damage. An epigenetic perspective. *Int. J. Environ. Res. Public. Health* **15**, 1971. <https://doi.org/10.3390/ijerph15091971> (2018).
11. Yan, T. et al. Acute morphine treatments alleviate tremor in 1-methyl-4-phenyl-1,2,3,6-tetrahydropyridine-treated monkeys. *PLoS One* **9**, 88404. <https://doi.org/10.1371/journal.pone.0088404> (2014).
12. Jenner, P. Parkinson's disease—the debate on the clinical phenomenology, aetiology, pathology and pathogenesis. *J. Parkinson's Disease* **3**, 1–11. <https://doi.org/10.3233/JPD-130175> (2013).
13. Sharma, N. K. Role of ionizing radiation in neurodegenerative diseases. *Front. Aging Neurosci.* **10**, 134. <https://doi.org/10.3389/fagi.2018.00134> (2018).
14. Langston, J. W. The MPTP story. *J. Parkinsons Dis.* **7**, 11–19. <https://doi.org/10.3233/JPD-179006> (2017).
15. Wang, J., Song, N., Jiang, H., Wang, J. & Xie, J. Pro-inflammatory cytokines modulate iron regulatory protein 1 expression and iron transportation through reactive oxygen/nitrogen species production in ventral mesencephalic neurons. *Biochim. Biophys. Acta* **1832**, 618–625. <https://doi.org/10.1016/j.bbadic.2013.01.021> (2013).
16. Betlazar, C., Middleton, R. J., Banati, R. B. & Liu, G. J. The impact of high and low dose ionising radiation on the central nervous system. *Redox Biol.* **9**, 144–156. <https://doi.org/10.1016/j.redox.2016.08.002> (2016).
17. Tagkalidou, N. et al. Motor and non-motor effects of acute MPTP in adult zebrafish: insights into parkinson's disease. *Int. J. Mol. Sci.* **26** (4), 1674. <https://doi.org/10.3390/ijms26041674> (2025).
18. Lam, C. S., Korzh, V. & Strahle, U. Zebrafish embryos are susceptible to the dopaminergic neurotoxin MPTP. *Eur. J. Neurosci.* **21**, 1758–1762. <https://doi.org/10.1111/j.1460-9568.2005.03988.x> (2005).
19. Unal, I. & Emelekli-Alturfan, E. Fishing for parkinson's disease: A review of the literature. *J. Clin. Neuroscience: Official J. Neurosurgical Soc. Australasia* **62**, 1–6. <https://doi.org/10.1016/j.jocn.2019.01.015> (2019).
20. Breton, C. V. et al. Exploring the evidence for epigenetic regulation of environmental influences on child health across generations. *Commun. Biol.* **4**, 769. <https://doi.org/10.1038/s42003-021-02316-6> (2021).
21. Si, J. et al. Effects of 12 C + 6 ion radiation and ferulic acid on the zebrafish (*Danio rerio*) embryonic oxidative stress response and gene expression. *Mutat. Res.* **745–746**, 26–33. <https://doi.org/10.1016/j.mrfmm.2013.03.007> (2013).
22. Williams, P. M. & Fletcher, S. Health effects of prenatal radiation exposure. *Am. Family Phys.* **82**, 488–493 (2010).
23. Tang, F. R. et al. Effects of continuous prenatal low dose rate irradiation on neurobehavior, hippocampal cellularity, messenger RNA and MicroRNA expression on B6C3F1 mice. *Cells* **13** (17), 1423. <https://doi.org/10.3390/cells13171423> (2024).
24. Westerfield, M. *The Zebrafish Book: A Guide for the Laboratory Use of Zebrafish* (University of Oregon, 1995).
25. Goody, M. F. et al. NAD + biosynthesis ameliorates a zebrafish model of muscular dystrophy. *PLoS Biol.* **10**, 1001409. <https://doi.org/10.1371/journal.pbio.1001409> (2012).
26. Ustundag, U. V. et al. White LED light exposure inhibits the development and Xanthophore pigmentation of zebrafish embryo. *Sci. Rep.* **9**, 10810. <https://doi.org/10.1038/s41598-019-47163-y> (2019).
27. Lowry, O. H., Rosebrough, N. J., Farr, A. L. & Randall, R. J. Protein measurement with the Folin phenol reagent. *J. Biol. Chem.* **193**, 265–275 (1951).
28. Yagi, K. Assay for blood plasma or serum. *Methods Enzymol.* **105**, 328–331. [https://doi.org/10.1016/s0076-6879\(84\)05042-4](https://doi.org/10.1016/s0076-6879(84)05042-4) (1984).
29. Miranda, K. M., Espey, M. G. & Wink, D. A. A rapid, simple spectrophotometric method for simultaneous detection of nitrate and nitrite. *Nitric Oxide: Biology and Chem.* **5**, 62–71. <https://doi.org/10.1006/niox.2000.0319> (2001).
30. Habig, W. H., Pabst, M. J. & Jakoby, W. B. Glutathione S-transferases. The first enzymatic step in mercapturic acid formation. *J. Biol. Chem.* **249**, 7130–7139 (1974).
31. Mylroie, A. A., Collins, H., Umbles, C. & Kyle, J. Erythrocyte superoxide dismutase activity and other parameters of copper status in rats ingesting lead acetate. *Toxicol. Appl. Pharmacol.* **82**, 512–520. [https://doi.org/10.1016/0041-008x\(86\)90286-3](https://doi.org/10.1016/0041-008x(86)90286-3) (1986).
32. Beutler, E. Glutathione: red cell metabolism. A manual biochemical method. *New York: Grune Stratton* **49**, 72–136. (1975).
33. Ellman, G. L., Courtney, K. D., Andres, V. Jr. & Feather-Stone, R. M. A new and rapid colorimetric determination of acetylcholinesterase activity. *Biochem. Pharmacol.* **7**, 88–95. [https://doi.org/10.1016/0006-2952\(61\)90145-9](https://doi.org/10.1016/0006-2952(61)90145-9) (1961).
34. Aebi, H. Catalase in vitro. *Methods Enzymol.* **105**, 121–126. [https://doi.org/10.1016/s0076-6879\(84\)05016-3](https://doi.org/10.1016/s0076-6879(84)05016-3) (1974).
35. Livak, K. J. & Schmittgen, T. D. Analysis of relative gene expression data using real-time quantitative PCR and the 2(-Delta Delta C(T)) Method. *Methods.* **25**, 402–8. <https://doi.org/10.1006/meth.2001.1262> (2001).
36. Teixidó, E., Piqué, E., Catalán, J. & Llobet, J. Assessment of developmental delay in the zebrafish embryo teratogenicity assay. *Toxicol. Vitro.* **27**, 469–478. <https://doi.org/10.1016/j.tiv.2012.07.010> (2013).
37. Sant, K. & Laragy, A. Zebrafish as a model for toxicological perturbation of yolk and nutrition in the early embryo. *Curr. Environ. Health Rep.* **5**, 125–133. <https://doi.org/10.1007/s40572-018-0183-2> (2018).
38. Ustundag, F. D. et al. 3-Pyridinylboronic acid normalizes the effects of 1-Methyl-4-phenyl-1,2,3,6-tetrahydropyridine exposure in zebrafish embryos. *Drug Chem. Toxicol.* **45**, 947–954. <https://doi.org/10.1080/01480545.2020.1795189> (2022).
39. Wiegand, J. et al. Triphenyl phosphate-induced pericardial edema in zebrafish embryos is dependent on the ionic strength of exposure media. *Environ. Int.* **172**, 107757. <https://doi.org/10.1016/j.envint.2023.107757> (2023).
40. Singh, J. & Patten, S. A. Modeling neuromuscular diseases in zebrafish. *Front. Mol. Neurosci.* **15**, 1054573. <https://doi.org/10.3389/fnmol.2022.1054573> (2022).
41. Cansiz, D., Ustundag, U. V., Unal, I., Alturfan, A. A. & Emelekli-Alturfan, E. Morphine attenuates neurotoxic effects of MPTP in zebrafish embryos by regulating oxidant/antioxidant balance and acetylcholinesterase activity. *Drug Chem. Toxicol.* **45**, 2439–2447. <https://doi.org/10.1080/01480545.2021.1957558> (2022).
42. Kollayan, B. Y. et al. Effects of low-dose ionizing radiation on the molecular pathways linking neurogenesis and autism spectrum disorders in zebrafish embryos. *Drug Chem. Toxicol.* **47**, 960–997. <https://doi.org/10.1080/01480545.2024.2318444> (2024).
43. Holschneider, D. P., Guo, Y., Roch, M., Norman, K. M. & Scrimin, O. U. Acetylcholinesterase inhibition and locomotor function after motor-sensory cortex impact injury. *J. Neurotrauma* **28**, 1909–1919. <https://doi.org/10.1089/neu.2011.1978> (2011).

44. Greenamyre, J. T. & Hastings, T. G. Biomedicine. Parkinson's–divergent causes, convergent mechanisms. *Science (New York)*. **304**, 1120–1122. (2004). <https://doi.org/10.1126/science.1098966>
45. Deas, E., Plun-Favreau, H. & Wood, N. W. PINK1 function in health and disease. *EMBO Mol. Med. Jun.* **1**, 152–165 (2009).
46. Di Maio, R. et al. LRRK2 activation in idiopathic Parkinson's disease. *Sci. Transl. Med.* **10** <https://doi.org/10.1126/scitranslmed.aar5429> (2018). eaar5429.
47. Takahashi-Niki, K. DJ-1-dependent protective activity of DJ-1-binding compound 23 against neuronal cell death in MPTP-treated mouse model of parkinson's disease. *J. Pharmacol. Sci.* **127**, 305–310. <https://doi.org/10.1016/j.jphs.2015.01.010> (2015).
48. Karagoz, A. et al. Panoramic dental x-ray exposure leads to oxidative stress, inflammation and apoptosis-mediated developmental defects in zebrafish embryos. *J. Stomatol. Oral Maxillofac. Surg.* **124**, 101661. <https://doi.org/10.1016/j.jormas.2023.101661> (2023).
49. Nishi, M., Takashima, H., Oka, T., Ohishi, N. & Yagi, K. Effect of x-ray irradiation on lipid peroxide levels in the rat submandibular gland. *J. Dent. Res.* **65**, 1028–1029. <https://doi.org/10.1177/00220345860650070701> (1986).
50. Finkel, T. Oxidant signals and oxidative stress. *Curr. Opin. Cell Biol.* **15**, 247–254. [https://doi.org/10.1016/s0955-0674\(03\)00002-4](https://doi.org/10.1016/s0955-0674(03)00002-4) (2003).
51. Valko, M., Rhodes, C. J., Moncol, J., Izakovic, M. & Mazur, M. Free radicals, metals and antioxidants in oxidative stress-induced cancer. *Chemico-Biol. Interact.* **160**, 1–40. <https://doi.org/10.1016/j.cbi.2005.12.009> (2006).
52. Kumar, H. et al. The role of free radicals in the aging brain and parkinson's disease: Convergence and parallelism. *Int J. Mol Sci.* **13**, 10478–10504. <https://doi.org/10.3390/ijms130810478> (2012).
53. Hirsch, E. C. Does oxidative stress participate in nerve cell death in parkinson's disease? *Eur. Neurol.* **33**, 52–59. <https://doi.org/10.1159/000118538> (1993).
54. Corongiu, F. P. et al. MPTP fails to induce lipid peroxidation in vivo. *Biochem. Pharmacol.* **36**, 2251–2253. [https://doi.org/10.1016/0006-2952\(87\)90587-9](https://doi.org/10.1016/0006-2952(87)90587-9) (1987).
55. Thiffault, C., Aumont, N., Quirion, R. & Poirier, J. Effect of MPTP and L-deprenyl on antioxidant enzymes and lipid peroxidation levels in mouse brain. *J. Neurochem.* **65**, 2725–2733. <https://doi.org/10.1046/j.1471-4159.1995.65062725.x> (1995).
56. Kojima, S. et al. Elevation of antioxidant potency in the brain of mice by low-dose gamma-ray irradiation and its effect on 1-methyl-4-phenyl-1,2,3,6-tetrahydropyridine (MPTP)-induced brain damage. *Free Radic Biol. Med.* **26**, 388–395. [https://doi.org/10.1016/s0891-5849\(98\)00200-7](https://doi.org/10.1016/s0891-5849(98)00200-7) (1999).
57. Xia, X. J., Lian, Y. G., Zhao, H. Y. & Xu, Q. L. Curcumin protects from oxidative stress and inhibits a-synuclein aggregation in MPTP induced parkinsonian mice. *Int. J. Clin. Exp. Med.* **9**, 2654–2665 (2016).
58. Wu, R. M., Chiueh, C. C., Pert, A. & Murphy, D. L. Apparent antioxidant effect of l-deprenyl on hydroxyl radical formation and nigral injury elicited by MPP+ in vivo. *Eur. J. Pharmacol.* **243**, 241–247. [https://doi.org/10.1016/0014-2999\(93\)90181-g](https://doi.org/10.1016/0014-2999(93)90181-g) (1993).
59. Rojas, P. & Rios, C. Increased striatal lipid peroxidation after intracerebroventricular MPP+ administration to mice. *Pharmacol. Toxicol.* **72**, 364–368. <https://doi.org/10.1111/j.1600-0773.1993.tb01345.x> (1993).
60. Moritake, T. et al. ESR spin trapping of hydroxyl radicals in aqueous solution irradiated with high-LET carbon-ion beams. *Radiat. Res.* **159**, 670–675. (2003).
61. Nakagawa, H., Ikota, N., Ozawa, T. & Kotake, Y. Dose- and time-dependence of radiation-induced nitric oxide formation in mice as quantified with electron paramagnetic resonance. *Nitric Oxide: Biology Chem.* **5**, 47–52. <https://doi.org/10.1006/niox.2000.0321> (2001).
62. Dede, S., Deger, Y., Kahraman, T. & Kilicpalp, D. Effects of x-ray radiation on oxidation products of nitric oxide in rabbits treated with antioxidant compounds. *Turkish J. Biochem.* **34**, 15–18 (2009).
63. Jackson-Lewis, V. & Smeyne, R. J. MPTP and SNpc DA neuronal vulnerability: role of dopamine, superoxide and nitric oxide in neurotoxicity. Minireview. *Neurotox. Res.* **7**, 193–202. <https://doi.org/10.1007/BF03036449> (2005).
64. Przedborski, S. et al. Role of neuronal nitric oxide in 1-methyl-4-phenyl-1,2,3,6-tetrahydropyridine (MPTP)-induced dopaminergic neurotoxicity. *Proc. Natl. Acad. Sci. U.S.A.* **93**, 4565–4571. <https://doi.org/10.1073/pnas.93.10.4565> (1996).
65. Xu, G. X. et al.  $\alpha$ B-crystallin malondialdehyde, superoxide dismutase, and lutathione peroxidase changes in x-ray irradiated rat lens. *Int. J. Ophthalmol.* **4**, 365–370. <https://doi.org/10.3980/j.issn.2222-3959.2011.04.08> (2011).
66. Zhou, R. et al. The effects of x-ray radiation on the eye development of zebrafish. *Hum. Exp. Toxicol.* **33**, 1040–1050. <https://doi.org/10.1177/0960327114522278> (2014).
67. Halliwell, B. & Gutteridge, J. M. Role of free radicals and catalytic metal ions in human disease: An overview. *Methods Enzymol.* **186**, 1–85. [https://doi.org/10.1016/0076-6879\(90\)86093-b](https://doi.org/10.1016/0076-6879(90)86093-b) (1990).
68. Comelekoglu, U. et al. Effect of low-level 1800 MHz radiofrequency radiation on the rat sciatic nerve and the protective role of paricalcitol. *Bioelectromagnetics* **39**, 631–643. <https://doi.org/10.1002/bem.22149> (2018).
69. Ma, Y. et al. Roles of oxidative stress in synchrotron radiation x-ray-induced testicular damage of rodents. *Int. J. Physiol. Pathophysiol. Pharmacol.* **4**, 108–114 (2012).
70. Rojas, P., Hidalgo, J., Ebadi, M. & Rios, C. Changes of Metallothionein I + II proteins in the brain after 1-methyl-4-phenylpyridinium administration in mice. *Prog. Neuro-psychopharmacol. Biol. Psychiatry* **24**, 143–154. [https://doi.org/10.1016/s0278-5846\(99\)00077-9](https://doi.org/10.1016/s0278-5846(99)00077-9) (2000).
71. Castro-Caldas, M. et al. Glutathione S-transferase Pi mediates MPTP-induced c-Jun N-terminal kinase activation in the nigrostriatal pathway. *Mol. Neurobiol.* **45**, 466–477. <https://doi.org/10.1007/s12035-012-8266-9> (2012).
72. Kumar, S., Prabodh, K. & Glutathione S-transferases: role in combating abiotic stresses including arsenic detoxification in plants. *Front. Plant Sci.* **9**, 751. <https://doi.org/10.3389/fpls.2018.00751> (2018).
73. Paithankar, J. G., Raghu, S. V. & Patil, R. K. Concomitant changes in radiation resistance and Trehalose levels during life stages of drosophila melanogaster suggest radio-protective function of Trehalose. *Int. J. Radiat. Biol.* **94**, 576–589. <https://doi.org/10.1080/0953002.2018.1460499> (2018).
74. Tierbach, A., Groh, K. J., Schönenberger, R., Schirmer, K. & Suter, M. J. Glutathione S-Transferase protein expression in different life stages of zebrafish (Danio rerio). *Toxicol. Sci.* **162**, 702–712. <https://doi.org/10.1093/toxsci/kfx293> (2018).
75. Aps, J. K. & Scott, J. M. Oblique lateral radiographs and bitewings: Estimation of organ doses in head and neck region with Monte Carlo calculations. *Dento Maxillo Fac. Radiol.* **43**, 20130419. <https://doi.org/10.1259/dmfr.20130419> (2014).

## Acknowledgements

None.

## Author contributions

Conception/Design of study: Ebru Emekli-Alturfan; Sebnem Ercalik Yalcinkaya; Ezgi Cahide Aydas Bayramov. Data Acquisition: Ezgi Cahide Aydas Bayramov; Merih Beler; Derya Cansiz, Ismail Unal; Gizem Egilmez; Selma Yaltkaya; Atakan Karagoz. Data Analysis/Interpretation: Ebru Emekli-Alturfan; Sebnem Ercalik Yalcinkaya; Ezgi Cahide Aydas Bayramov; Hüseyin Gündüz. Drafting Manuscript: Sebnem Ercalik Yalcinkaya; Ezgi Cahide Aydas Bayramov. Critical Revision of Manuscript: Ebru Emekli-Alturfan, Sebnem Ercalik Yalcinkaya. Supervision: Ebru Emekli-Alturfan; Sebnem Ercalik Yalcinkaya.

## Funding

This study was supported by Marmara University Scientific Research Project Unit (BAPKO) number of 10981.

## Declarations

### Competing interests

The authors declare no competing interests.

### Ethical approval

Currently, the European Commission Directive 2010/63/EU, permits experimentation in fish embryos at earliest life stages without being regulated as animal experiments; zebrafish are considered models *in vitro* until 120 hpf (<http://data.europa.eu/eli/dir/2010/63/2019-06-26>; accessed 21 May 2025 EFSA opinion: <https://doi.org/10.2903/j.efsa.2005.292>; accessed 21 May 2025).

### Consent to participate

All the authors have agreed for authorship, read and approved the manuscript, and given consent to participate.

### Consent for publication

All the authors have agreed for authorship, read and approved the manuscript, and given consent for publication.

### Additional information

**Correspondence** and requests for materials should be addressed to S.E.Y.

**Reprints and permissions information** is available at [www.nature.com/reprints](http://www.nature.com/reprints).

**Publisher's note** Springer Nature remains neutral with regard to jurisdictional claims in published maps and institutional affiliations.

**Open Access** This article is licensed under a Creative Commons Attribution-NonCommercial-NoDerivatives 4.0 International License, which permits any non-commercial use, sharing, distribution and reproduction in any medium or format, as long as you give appropriate credit to the original author(s) and the source, provide a link to the Creative Commons licence, and indicate if you modified the licensed material. You do not have permission under this licence to share adapted material derived from this article or parts of it. The images or other third party material in this article are included in the article's Creative Commons licence, unless indicated otherwise in a credit line to the material. If material is not included in the article's Creative Commons licence and your intended use is not permitted by statutory regulation or exceeds the permitted use, you will need to obtain permission directly from the copyright holder. To view a copy of this licence, visit <http://creativecommons.org/licenses/by-nc-nd/4.0/>.

© The Author(s) 2025